Coupled-channel optical calculation of electron-hydrogen scattering: Elastic scattering from 0.5 to 30 eV

Igor Bray, Dmitry A. Konovalov, and Ian E. McCarthy
Electronic Structure of Materials Centre, School of Physical Sciences, The Flinders University of South Australia, G.P.O. Box 2100, Adelaide 5001, Australia
(Received 21 January 91)

A coupled-channel optical method for electron–atomic-hydrogen scattering is presented in a form that treats both the projectile and the target electrons symmetrically. Elastic differential cross sections are calculated at a range of energies from 0.5 to 30 eV and are found to be in complete agreement with the absolute measurements of Williams [J. Phys. B **8**, 1683 (1975); **8**, 2191 (1975)]. Total and total ionization cross sections are also presented.

I. INTRODUCTION

The electron–atomic-hydrogen scattering problem is one of the most fundamental problems in theoretical atomic physics. As the hydrogen wave functions are known exactly and a large body of experimental data is available for various aspects of this problem, it serves as an ideal test of any electron-atom scattering theory.

One approach to electron-atom scattering is the coupled-channel optical (CCO) method. This has proved to be successful for a number of atoms; see, for example, hydrogen,[1,2] helium,[3] and argon.[4] In this approach to electron-atom scattering a finite set of channels (P space) are treated explicitly via the coupled channels formalism, while the rest of the channels (Q space), including the target continuum, are taken into account indirectly through a complex nonlocal polarization potential. This potential, together with the first-order potentials of the explicitly treated channels, forms the optical potential.

The CCO approach of Bray, Madison, and McCarthy[1] has proved to be successful for electron-hydrogen scattering at intermediate energies (30–400 eV). In this approach P and Q projection operators are only defined in the target space. This leads to the spin-dependent space-exchange operator $(-1)^S P_r$ appearing in the Q-projected Green's function inside the polarization potential. In the calculation of this Green's function the spin-dependent part was dropped, resulting in a nonsymmetric treatment of the two electrons. We have found that the results are not sensitive to this approximation at incident projectile energies of at least 54 eV.[5] However, this approximation breaks down for low energy, where symmetry properties become more important.

The aim of this paper is to expand our theory to low energies (< 30 eV) and to test this theory by applying it to entrance-channel phenomena for scattering of electrons on atomic hydrogen. There is a large number of experimental absolute elastic differential cross sections at these energies by Williams[6,7] as well as in a recent experiment of Shyn and Cho.[8] There are also measurements of the total ionization cross section for energies above the ionization threshold[9] as well as the semiempirical data of de Heer, McDowell, and Wagenaar[10] for various total inelastic cross sections. Therefore we have plenty of information to test our theory.

In Sec. II we present the formal theory of our CCO method. This theory has been extended to describe low-energy scattering as well as high-energy scattering. Here we use projection operators P and Q that are symmetric in the space of the two electrons. As a result the Q-projected Green's function inside the polarization potential does not contain spin dependence. The two electrons are treated in a symmetric manner everywhere. In Sec. III we discuss the approximations used in calculating the Q-projected Green's function and examine the effect on the total and total ionization cross sections. In Sec. IV the elastic differential cross sections are presented at a range of energies 0.5–30 eV. These are calculated using a CCO model that has $1s$ in P space and the rest in Q space (1CCO). We use the notation nCCO for a calculation that has the lowest n target states in P space and the rest in Q space.

Our approach to the CCO method has been shown to be internally consistent.[1,5] By this we mean that the P space need only contain channels for which we wish to compare with experiment, since the results are the same irrespective of whether other discrete channels are included in P space or Q space. Thus, for the $1s$ entrance channel we only need to do a 1CCO calculation as it is an order of magnitude faster than say a 3CCO calculation where P space consists of $1s$, $2s$, and $2p$. A typical 1CCO calculation takes 5 h on a 5 Mflop CPU (Solbourne 5/501). Elastic differential cross sections for higher energies with this model are consistent with our previous work[1] and so are not discussed here.

II. FORMAL DERIVATION OF THE CCO METHOD

The total nonrelativistic Hamiltonian for the electron-hydrogen scattering problem is

$$H = K_1 + K_2 + v_1 + v_2 + v_3, \tag{1}$$

where K_1 and K_2 are the kinetic-energy operators of electrons 1 and 2 with the corresponding electron-nucleus potentials v_1 and v_2. The electron-electron potential is v_3. In coordinate space representation

$$v_1(r_1) = -\frac{1}{r_1}, \quad v_2(r_2) = -\frac{1}{r_2}, \quad v_3(\mathbf{r}_1, \mathbf{r}_2) = \frac{1}{|\mathbf{r}_1 - \mathbf{r}_2|}. \tag{2}$$

As the mass of the nucleus is very much greater than that of the electron, the center of mass frame is taken to be the nucleus.

The Schrödinger equation for electron-hydrogen scattering is

$$(E^{(+)} - H) \mid \Psi^{(+)S}_{i_0\mathbf{k}_0}\rangle = 0, \tag{3}$$

with the corresponding boundary condition

$$\lim_{r_1\to\infty} \Psi^{(+)S}_{i_0\mathbf{k}_0}(\mathbf{r}_1, \mathbf{r}_2) = (2\pi)^{-3/2} \exp(i\mathbf{k}_0 \cdot \mathbf{r}_1)\phi_{i_0}(\mathbf{r}_2), \tag{4}$$

where the superscript (+) indicates outgoing spherical wave boundary conditions. The incident momentum of the projectile electron is $\mathbf{k}_0$ and the incident target ground state is ϕ_{i_0}. The total spin S is a good quantum number in the nonrelativistic quantum theory for two electrons, and describes the symmetry property of the total wave function

$$\Psi^{(+)S}_{i_0\mathbf{k}_0}(\mathbf{r}_1, \mathbf{r}_2) = (-1)^S \Psi^{(+)S}_{i_0\mathbf{k}_0}(\mathbf{r}_2, \mathbf{r}_1). \tag{5}$$

We drop the superscript (+) from $\Psi^{(+)S}_{i_0\mathbf{k}_0}$ to simplify the notation.

The coordinate space of the two electrons is divided into two by the projection operators P and Q such that

$$P + Q = I, \quad PQ = QP = 0, \quad P^2 = P, \quad Q^2 = Q. \tag{6}$$

We define P and Q using one-electron projection operators P_α and Q_α, where $\alpha = 1, 2$ is the electron space label, by[11]

$$P_\alpha + Q_\alpha = I_\alpha, \quad P = P_1 I_2 + I_1 P_2 - P_1 P_2, \quad Q = Q_1 Q_2, \tag{7}$$

where

$$P_\alpha = \sum_{\phi_i \in P_\alpha} |\phi_i\rangle\langle\phi_i|, \tag{8}$$

and where

$$(K_\alpha + v_\alpha - \epsilon_i)\,\phi_i(\mathbf{r}_\alpha) = 0. \tag{9}$$

This definition of P and Q satisfies (6). Using (4) with $\phi_{i_0} \in P_\alpha$ we have

$$\lim_{r_1\to\infty} P\Psi^S_{i_0\mathbf{k}_0}(\mathbf{r}_1, \mathbf{r}_2) = \lim_{r_1\to\infty} \Psi^S_{i_0\mathbf{k}_0}(\mathbf{r}_1, \mathbf{r}_2), \tag{10}$$

$$\lim_{r_1\to\infty} Q\Psi^S_{i_0\mathbf{k}_0}(\mathbf{r}_1, \mathbf{r}_2) = 0. \tag{11}$$

From (5) we have

$$P\Psi^S_{i_0\mathbf{k}_0}(\mathbf{r}_1, \mathbf{r}_2) = (-1)^S P\Psi^S_{i_0\mathbf{k}_0}(\mathbf{r}_2, \mathbf{r}_1). \tag{12}$$

Inserting $P + Q$ in (3) and premultiplying by P and Q, respectively, we have

$$P(E^{(+)} - H)P \mid \Psi^S_{i_0\mathbf{k}_0}\rangle = PHQ \mid \Psi^S_{i_0\mathbf{k}_0}\rangle, \tag{13}$$

$$Q(E^{(+)} - H)Q \mid \Psi^S_{i_0\mathbf{k}_0}\rangle = QHP \mid \Psi^S_{i_0\mathbf{k}_0}\rangle. \tag{14}$$

Using the boundary condition (11) we can write

$$Q \mid \Psi^S_{i_0\mathbf{k}_0}\rangle = QG_Q(E^{(+)})QHP \mid \Psi^S_{i_0\mathbf{k}_0}\rangle, \tag{15}$$

where

$$Q(E^{(+)} - H)QG_Q(E^{(+)}) = Q \tag{16}$$

defines $G_Q(E^{(+)})$, the Q-projected Green's function. Thus we can write the P-projected Schrödinger equation

$$P(E^{(+)} - H - V_Q)P \mid \Psi^S_{i_0\mathbf{k}_0}\rangle = 0, \tag{17}$$

where

$$V_Q = Pv_3QG_Q(E^{(+)})Qv_3P \tag{18}$$

is the complex nonlocal polarization potential, and where we used the identity $PHQ = Pv_3Q$.

To solve (17) with the boundary condition (10) and symmetry property (12) we use the multichannel expansion

$$P\Psi^S_{i_0\mathbf{k}_0}(\mathbf{r}_1, \mathbf{r}_2) \approx \sum_{\phi_i \in P} \left[F^S_i(\mathbf{r}_1)\phi_i(\mathbf{r}_2) + (-1)^S F^S_i(\mathbf{r}_2)\phi_i(\mathbf{r}_1)\right], \tag{19}$$

where ϕ_i are the hydrogen wave functions.

Let

$$\psi^S_{i_0\mathbf{k}_0}(\mathbf{r}_1, \mathbf{r}_2) = \sum_{\phi_i \in P_2} F^S_i(\mathbf{r}_1)\phi_i(\mathbf{r}_2) \tag{20}$$

and P_r be the space exchange operator. Then we can write

$$P\Psi^S_{i_0\mathbf{k}_0}(\mathbf{r}_1, \mathbf{r}_2) \approx \left[1 + (-1)^S P_r\right] \psi^S_{i_0\mathbf{k}_0}(\mathbf{r}_1, \mathbf{r}_2), \tag{21}$$

and replace (17) by

$$P[E^{(+)} - H - V_Q + (-1)^S(E^{(+)} - H - V_Q)P_r]P \mid \psi^S_{i_0\mathbf{k}_0}\rangle = 0, \tag{22}$$

where $\psi^S_{i_0\mathbf{k}_0}(\mathbf{r}_1, \mathbf{r}_2)$ satisfies the boundary condition (4). The symmetry properties of the total wave function (5) and (12) are now inside the above equation.

We split H

$$H = K + V, \quad K = K_1 + K_2 + v_2, \quad V = v_1 + v_3, \tag{23}$$

to get

$$P(E^{(+)} - K)P \mid \psi^S_{i_0\mathbf{k}_0}\rangle = PV^S_Q P \mid \psi^S_{i_0\mathbf{k}_0}\rangle, \tag{24}$$

where

$$V^S_Q = P[V + V_Q + (-1)^S(H + V_Q - E^{(+)})P_r]P \tag{25}$$

is known as the optical potential. From (20) we require the solution of (24) to be only in P_2 space. Therefore we multiply (24) by P_2 to get

$$P_2(E^{(+)} - K)P_2 \mid \psi^S_{i_0\mathbf{k}_0}\rangle = P_2V^S_Q P_2 \mid \psi^S_{i_0\mathbf{k}_0}\rangle, \tag{26}$$

where we used the identities

$$P_2P = P_2, \quad P_2(E^{(+)} - K)P = P_2(E^{(+)} - K)P_2, \tag{27}$$

as well as

$$\mid \psi^S_{i_0\mathbf{k}_0}\rangle = P \mid \psi^S_{i_0\mathbf{k}_0}\rangle = P_2 \mid \psi^S_{i_0\mathbf{k}_0}\rangle. \tag{28}$$

By making the P_2 projection (26) has not lost the required symmetry. It contains the same information as (24).[11]

Using boundary condition (4), Eq. (26) can be written in integral form

$$\mid \psi^S_{i_0\mathbf{k}_0}\rangle = \mid \phi_{i_0}\mathbf{k}_0\rangle + \frac{1}{P_2\,(E^{(+)} - K)\,P_2}P_2V^S_Q P_2 \mid \psi^S_{i_0\mathbf{k}_0}\rangle, \tag{29}$$

where

$$\langle \mathbf{r}_1\mathbf{r}_2 \mid \phi_i\mathbf{k}\rangle = (2\pi)^{-3/2}\exp(i\mathbf{k}\cdot\mathbf{r}_1)\phi_i(\mathbf{r}_2), \tag{30}$$

and therefore

$$P_2 \mid \phi_i\mathbf{k}\rangle = \mid \phi_i\mathbf{k}\rangle, \quad \phi_i \in P_2 \tag{31}$$

and

$$P_2\,(E - K)\,P_2 \mid \phi_{i_0}\mathbf{k}_0\rangle = 0, \quad \phi_{i_0} \in P_2 \tag{32}$$

define the on-shell energy. The P_2-projected T matrix is defined by[1]

$$\langle \mathbf{k}\phi_i \mid T^S \mid \phi_{i_0}\mathbf{k}_0\rangle = \langle \mathbf{k}\phi_i \mid V^S_Q P_2 \mid \psi^S_{i_0\mathbf{k}_0}\rangle. \tag{33}$$

Premultiplying (29) by $\langle \mathbf{k}\phi_i \mid V^S_Q$ we have the Lippman-Schwinger equation for the T matrix

$$\langle \mathbf{k}\phi_i \mid T^S \mid \phi_{i_0}\mathbf{k}_0\rangle = \langle \mathbf{k}\phi_i \mid V^S_Q \mid \phi_{i_0}\mathbf{k}_0\rangle + \sum_{\phi_{i'}\in P_2}\int d^3k' \frac{\langle \mathbf{k}\phi_i \mid V^S_Q \mid \phi_{i'}\mathbf{k}'\rangle}{(E^{(+)} - \epsilon_{i'} - k'^2/2)} \times \langle \mathbf{k}'\phi_{i'} \mid T^S \mid \phi_{i_0}\mathbf{k}_0\rangle. \tag{34}$$

Evaluation of the CCO Lippman-Schwinger equation

We evaluate (34) using partial wave representation defining the radial wave functions explicitly by

$$\langle \mathbf{r}_1\mathbf{r}_2 \mid \phi_i\mathbf{k}\rangle \equiv \langle \mathbf{r}_1\mathbf{r}_2 \mid \phi_{nlm}\mathbf{k}\rangle \tag{35}$$

$$= (2/\pi)^{1/2}(kr_1)^{-1} \times \sum_{L,M} i^L U_L(kr_1)Y^*_{LM}(\hat{\mathbf{k}})Y_{LM}(\hat{\mathbf{r}}_1) \times r_2^{-1}u_{nl}(r_2)Y_{lm}(\hat{\mathbf{r}}_2), \tag{36}$$

where $U_L(x) = xj_L(x)$ are the Riccati-Bessel functions and $u_{nl}(r)$ are the hydrogen radial wave functions. The reduced V (or T) matrix elements are given by

$$\langle Lln \| V^{SJ}_Q(k,k') \| n'l'L'\rangle = \sum_{M,m} C^{MmM_J}_{LlJ}C^{M'm'M_J}_{L'l'J}\int d\hat{\mathbf{k}}\int d\hat{\mathbf{k}}' Y^*_{LM}(\mathbf{k})Y_{L'M'}(\mathbf{k}')\langle \mathbf{k}\phi_{nlm} \mid V^S_Q \mid \phi_{n'l'm'}\mathbf{k}'\rangle, \tag{37}$$

where J is the total orbital angular momentum and C denotes a Clebsch-Gordan coefficient. The partial-wave Lippman-Schwinger equation is

$$\langle Lln \| T^{SJ}(k,k_0) \| n_0l_0L_0\rangle = \langle Lln \| V^{SJ}_Q(k,k_0) \| n_0l_0L_0\rangle + \sum_{\substack{n'l'\in P_2\\ L'}}\int dk'k'^2 \frac{\langle Lln \| V^{SJ}_Q(k,k') \| n'l'L'\rangle}{(E^{(+)} - \epsilon_{i'} - k'^2/2)}\langle L'l'n' \| T^{SJ}(k',k_0) \| n_0l_0L_0\rangle. \tag{38}$$

The method of solution of the above equation is discussed in detail by McCarthy and Stelbovics.[12] There they also present the relationship between the T matrix and various observable quantities.

To evaluate the reduced V matrix elements of (38) we expand (25)

$$\langle Lln \| V^{SJ}_Q(k,k') \| n'l'L'\rangle = \langle J, Llnk \| v_1 + v_3 \| k'n'l'L', J\rangle + (-1)^S\langle J, Llnk \| (v_3 + \epsilon_n + \epsilon_{n'} - E)P_r \| k'n'l'L', J\rangle + \langle J, Llnk \| V_Q[1 + (-1)^S P_r] \| k'n'l'L', J\rangle. \tag{39}$$

An explicit expansion of the first two terms can be found in McCarthy and Stelbovics.[12] In order to evaluate the last term we need to find the Q-projected Green's function of (16).

III. THE Q-PROJECTED GREEN'S FUNCTION

The definition of the Q-projected Green's function differs from our previous work[1,5] with nonsymmetric P and Q by the fact that the space exchange operator P_r does not appear in (16). In a partial wave expansion (16) becomes

$$\langle J, L'l'n' \| Q(E^{(+)} - H)QG_Q(E^{(+)}) \| nlL, J\rangle = \langle J, L'l'n' \| Q \| nlL, J\rangle, \quad (40)$$

where the reduced matrix-element notation indicates integration over the $\hat{\mathbf{r}}_1$ and $\mathbf{r}_2$ coordinates with

$$\begin{aligned}\langle \hat{\mathbf{r}}_1, \mathbf{r}_2 \| nlL, J\rangle &= r_2^{-1} u_{nl}(r_2)\langle \hat{\mathbf{r}}_1, \hat{\mathbf{r}}_2 \| lL, J\rangle \\ &= r_2^{-1} u_{nl}(r_2) \sum_{M,m} C_{LlJ}^{MmM_J} Y_{LM}(\hat{\mathbf{r}}_1) Y_{lm}(\hat{\mathbf{r}}_2). \end{aligned} \quad (41)$$

By taking the integral over r_2 we break symmetry between the two electron spaces, which will be restored later by explicit symmetrization.

The Q projection operator in partial wave representation is

$$Q = \sum_{J'} \sum_{\substack{L\in Q_1 \\ l\in Q_2}} \| lL, J'\rangle\langle J', Ll \| Q_{1L} Q_{2l}, \quad (42)$$

where for $l \in Q_\alpha$ $(\alpha = 1, 2)$

$$\begin{aligned} Q_{\alpha l} &= \sum_{n\in Q_\alpha} | u_{nl}\rangle\langle u_{nl} | \\ &= \sum_{n\in Q_\alpha^-} | u_{nl}\rangle\langle u_{nl} | + \int_0^\infty dp\, p^2 \, | u_l(p)\rangle\langle u_l(p) | \\ &\approx \sum_{n\in Q_\alpha^-} | u_{nl}\rangle\langle u_{nl} | + \sum_{n\in Q_\alpha^+} w_n p_n^2 \, | u_l(p_n)\rangle\langle u_l(p_n) | . \end{aligned} \quad (43)$$

Here we have subdivided Q_α space into two parts: Q_α^- is the space of negative energy (bound) hydrogen states u_{nl}, and Q_α^+ is the space of positive energy (continuum) hydrogen states $u_l(p)$. The integral over the continuum has been replaced by a quadrature rule.

Using (42), with $n, n', l, l' \in Q_2$ and $L, L' \in Q_1$ in (40), we get

$$\sum_{n'',l''\in Q_2} \sum_{L''\in Q_1} \langle J, L'l'n' \| Q_{1L'}(E^{(+)} - H)Q_{1L''} \| n''l''L'', J\rangle\langle J, L''l''n'' \| G_Q(E^{(+)}) \| nlL, J\rangle = \hat{\delta}_{n'n}\delta_{L'L}\delta_{l'l}Q_{1L}, \quad (44)$$

where

$$\hat{\delta}_{n'n} = \begin{cases} \delta_{n'n}, & n \in Q_2^- \\ p_n^{-2}\delta(p_{n'} - p_n), & n \in Q_2^+. \end{cases} \quad (45)$$

Using (23) we have

$$\begin{aligned}\langle J, L'l'n' \| Q_{1L'}(E^{(+)} - H)Q_{1L''} \| n''l''L'', J\rangle &= Q_{1L'}(E_n^{(+)} - K_{1L'} - v_1)Q_{1L'}\hat{\delta}_{n''n'}\delta_{L''L'}\delta_{l''l'} \\ &\quad - Q_{1L'}\langle J, L'l'n' \| v_3 \| n''l''L'', J\rangle Q_{1L''}, \end{aligned} \quad (46)$$

where

$$K_{1L} = -\frac{1}{2}\frac{d^2}{dr_1^2} + \frac{1}{2}\frac{L'(L'+1)}{r_1^2} \quad (47)$$

and

$$E_n^{(+)} = E^{(+)} - \epsilon_n. \quad (48)$$

We make the weak coupling in Q-space approximation for the reduced v_3 matrix elements in (46)

$$\langle J, L'l'n' \| v_3 \| n''l''L'', J\rangle = \hat{\delta}_{n''n'}\delta_{L''L'}\delta_{l''l'}V_{1n'l'L'}^J(r_1). \quad (49)$$

The subscript 1 on $V_{1n'l'L'}^J$ indicates that this potential acts in r_1 space. The required Green's function is then given by

$$\langle J, L'l'n' \| G_Q(E^{(+)}) \| nlL, J\rangle \approx \hat{\delta}_{n'n}\delta_{L'L}\delta_{l'l}Q_{1L}G_{1nlL}^J(E_n^{(+)})Q_{1L}, \quad (50)$$

where $G_{1nlL}^J(E_n^{(+)})$ is defined by

$$(E_n^{(+)} - K_{1L} - v_1 - V_{1nlL}^J)G_{1nlL}^J(E_n^{(+)}) = I. \quad (51)$$

The solution to the above equation is

$$G_{1nlL}^J(E_n^{(+)}, r_1', r_1) = -k_n^{-1} f_{nlL}^J(k_n r_<)[g_{nlL}^J(k_n r_>) + i f_{nlL}^J(k_n r_>)], \quad (52)$$

where f and g denote, respectively, the regular and irregular solutions of

$$(E_n^{(+)} - K_{1L} - v_1 - V_{1nlL}^J) \times \begin{Bmatrix} f_{nlL}^J(r_1) \\ g_{nlL}^J(r_1) \end{Bmatrix} = 0, \quad (53)$$

with appropriate boundary conditions, and where k_n is defined by $k_n^2/2 = E_n$.

Having defined $G_{1nlL}^J(E_n^{(+)})$ we write our approximation to the Q-projected Green's function $G_Q(E^{(+)})$ as

$$G_Q(E^{(+)}) \approx \tfrac{1}{2} \sum_{\substack{J \\ n,l\in Q_2 \\ L\in Q_1}} ||nlL,J\rangle G^J_{1nlL}(E_n^{(+)})\langle J,Lln|| + \tfrac{1}{2} \sum_{\substack{J \\ n,l\in Q_1 \\ L\in Q_2}} ||nlL,J\rangle G^J_{2nlL}(E_n^{(+)})\langle J,Lln||, \tag{54}$$

where in order to ensure the initial symmetry in Q space we have explicitly symmetrized $G_Q(E^{(+)})$ in terms of its nonsymmetric parts. The factor of a half avoids double counting.

The final form of the last term of (39) is then

$$\begin{aligned}
&\langle J,L''l''n''k''||V_Q[1+(-1)^S P_r]||k'n'l'L',J\rangle \\
&= \tfrac{1}{2} \sum_{\substack{n,l\in Q_2 \\ L\in Q_1}} \int_0^\infty dr_1 \int_0^\infty dr_1' \langle J,L''l''n''k''||v_3||nlL,J\rangle G^J_{1nlL}(E_n^{(+)},r_1',r_1)\langle J,Lln||v_3[1+(-1)^S P_r]||k'n'l'L',J\rangle \\
&+ \tfrac{1}{2} \sum_{\substack{n,l\in Q_1 \\ L\in Q_2}} \int_0^\infty dr_2 \int_0^\infty dr_2' \langle J,L''l''n''k''||v_3||nlL,J\rangle G^J_{2nlL}(E_n^{(+)},r_2',r_2)\langle J,Lln||v_3[1+(-1)^S P_r]||k'n'l'L',J\rangle.
\end{aligned} \tag{55}$$

In order to calculate $G^J_{1nlL}(E_n^{(+)})$ we first need to define V^J_{1nlL} in (53). For $n,l \in Q_2^-$ we have, using (49)

$$V^J_{1nlL} = \langle J,Lln||v_3||nlL,J\rangle, \tag{56}$$

which in coordinate representation is

$$V^J_{1nlL}(r_1) = (2l+1)(2L+1)(-1)^J \sum_\lambda \begin{Bmatrix} l & L & J \\ L & l & \lambda \end{Bmatrix} \begin{pmatrix} l & \lambda & l \\ 0 & 0 & 0 \end{pmatrix} \begin{pmatrix} L & \lambda & L \\ 0 & 0 & 0 \end{pmatrix} \int_0^\infty dr_2 \frac{r_<^\lambda}{r_>^{\lambda+1}} [u_{nl}(r_2)]^2. \tag{57}$$

This approach to the Q^- part of $G_Q(E^{(+)})$ contains the weak coupling in Q^--space approximation, which involves taking just the diagonal part of v_3 in the calculation of the Green's function. These diagonal matrix elements exist since the functions u_{nl} in (57) are the hydrogen bound states for $n,l \in Q_2^-$. However, for $n,l \in Q_2^+$ these functions are the hydrogen continuum functions and so the integral in (57) does not exist. For the Q_2^+ part of $G_Q(E^{(+)})$ we consider two approximations: $V^J_{1nlL}(r_1) = 0$ and $V^J_{1nlL}(r_1) = 1/r_1$.

The approximations for Q^- space may be checked internally[5] by, for example, comparing the results of a 3CC calculation with $1s$, $2s$, and $2p$ explicitly coupled in P space with the 1CCO calculation that has $1s$ in P space and $2s$ and $2p$ in Q^- space. However, there is no such direct check of the approximations for Q^+ space. To test these approximations we compare with experimental total ionization cross sections[9] (Fig. 1) and the semiempirical data for the total cross sections of de Heer, McDowell, and Wagenaar[10] (Table I).

The total cross section σ_t depends only on the T-matrix elements for the entrance channel and is therefore calculated by the 1CCO method. It includes the cross section for exciting nonelastic channels at incident energies above their thresholds. It therefore directly tests our approximation for the entire Q space, including the continuum Q^+.

The total ionization cross section σ_i can be approximately calculated by the present theory in which P space

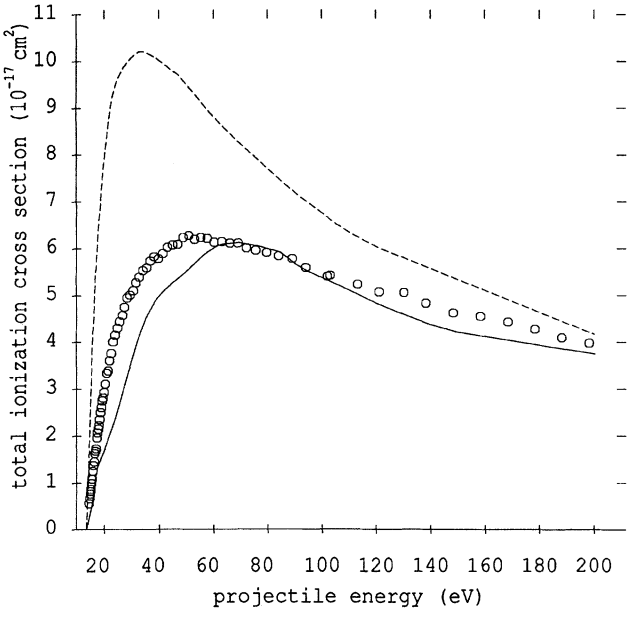

FIG. 1. Total ionization cross sections of atomic hydrogen by electron impact. The solid line is the 1CCO calculation with $V^J_{1nlL}(r_1) = 1/r_1$ (free Green's function) in the continuum, and the dashed line with $V^J_{1nlL}(r_1) = 0$ (Coulomb Green's function) in the continuum. The experimental points o are due to Shah, Elliot, and Gilbody (Ref. 9).

TABLE I. Integrated elastic (σ_e) and total (σ_t) cross sections (in units of πa_0^2) at 20 and 30 eV calculated using the 1CCO model with a free-particle Green's function in the continuum, see text. The semiempirical data (σ^{se}) are due to de Heer, McDowell, and Wagenaar (Ref. 10). The adopted values for σ_t^{se} are given.

Energy (eV)	σ_e	σ_e^{se}	σ_t	σ_t^{se}
20	3.30	3.35±0.3	4.69	4.57±0.5
30	2.04	2.01±0.2	3.66	4.05±0.4

contains the $1s$ state and $Q = Q_1^+ Q_2^+$, i.e., only the second sum in (43) is used. The effect of Q^- space on the ionization is completely ignored.

In our earlier higher-energy work[1] we took $V^J_{1nlL}(r_1) = 0$ when both electrons are in the continuum. This means that both electrons are then treated as hydrogen continuum waves, i.e., Coulomb waves. This approximation has proved to work well for $(e,2e)$ differential cross sections observed in a limited range of the kinematic space,[13] but it leads to very high total ionization cross sections for smaller energies and so overestimates total cross sections at these energies[1] (see Table I of Ref. 1).

In this work we make the approximation $V^J_{1nlL}(r_1) = 1/r_1$ when both electrons are in the continuum. This leads to the free-particle Green's function. One of the electrons is treated as a plane wave while the other is represented by a continuum state of the target. This is done in a symmetric manner since the symmetrization has been done explicitly in (54).

The free Green's function gives a much better estimate of σ_i than the Coulomb Green's function, although the estimate is now less than the experiment below 60 eV. However, at these energies it is not clear that the effect of Q^- space on ionization is negligible. We therefore consider the direct calculation of σ_t as a better test of the approximation for the Green's function, since the Q^+ approximations are tested together with the Q^- approximations. Comparison with the adopted semiempirical values of de Heer, McDowell, and Wagenaar[10] in Table I shows that σ_t is obtained within the quoted 10% uncertainty.

Numerical convergence in the polarization matrix elements to less than 1% was achieved by taking in (43) $n = 2,...,10$ and $l = 0,1,2,3$ for Q^-, and 30 continuum integration points p_n and $l = 0,...,10$ in Q^+. Numerical convergence in differential, total, and total ionization cross sections to less than 1% was achieved by taking up to 80 partial waves J in (38).

IV. ELASTIC DIFFERENTIAL CROSS SECTIONS

We have calculated the elastic differential cross sections at a range of energies (Table II) chosen from the tables of Williams.[6,7] These results were achieved using

TABLE II. Elastic differential cross sections ($a_0^2\,\mathrm{sr}^{-1}$) calculated using the 1CCO model at a range of energies (eV) at angles θ (deg). The integrated elastic σ_e and the total σ_t cross sections are in πa_0^2. Square brackets denote powers of 10.

θ (deg) \ Energy (eV)	0.582	1.207	2.171	3.423	4.889	6.691	8.704	12.0	20.0	30.0
10	5.30	3.98	4.19	5.20	6.34	7.17	7.68	7.15	6.44	5.56
15	5.36	4.00	4.04	4.90	5.78	6.48	6.83	6.20	5.16	4.10
20	5.44	4.03	3.90	4.59	5.28	5.84	6.04	5.35	4.09	2.99
25	5.55	4.07	3.78	4.30	4.82	5.25	5.31	4.60	3.23	2.19
30	5.68	4.13	3.68	4.03	4.41	4.71	4.66	3.95	2.56	1.63
35	5.82	4.20	3.61	3.79	4.04	4.21	4.09	3.39	2.04	1.25
40	5.98	4.29	3.56	3.58	3.71	3.77	3.59	2.92	1.65	9.78[-1]
45	6.14	4.40	3.53	3.41	3.41	3.38	3.16	2.51	1.36	7.87[-1]
50	6.32	4.52	3.54	3.26	3.16	3.04	2.78	2.17	1.13	6.46[-1]
55	6.50	4.66	3.57	3.15	2.95	2.75	2.47	1.88	9.57[-1]	5.40[-1]
60	6.68	4.81	3.62	3.07	2.77	2.51	2.20	1.64	8.20[-1]	4.57[-1]
70	7.05	5.15	3.79	3.01	2.53	2.14	1.78	1.27	6.21[-1]	3.37[-1]
80	7.43	5.53	4.04	3.07	2.41	1.91	1.50	1.01	4.90[-1]	2.56[-1]
90	7.80	5.94	4.36	3.22	2.41	1.79	1.33	8.38[-1]	4.00[-1]	1.99[-1]
100	8.16	6.37	4.73	3.46	2.50	1.77	1.25	7.34[-1]	3.38[-1]	1.60[-1]
110	8.51	6.80	5.14	3.76	2.67	1.83	1.25	6.87[-1]	2.95[-1]	1.33[-1]
120	8.82	7.21	5.57	4.10	2.90	1.95	1.31	6.88[-1]	2.66[-1]	1.14[-1]
130	9.10	7.59	5.99	4.46	3.16	2.11	1.42	7.28[-1]	2.45[-1]	1.01[-1]
140	9.32	7.91	6.37	4.79	3.42	2.28	1.55	7.98[-1]	2.31[-1]	9.18[-2]
150	9.49	8.17	6.68	5.08	3.66	2.45	1.68	8.82[-1]	2.21[-1]	8.56[-2]
σ_e	30.9	24.2	18.9	15.2	12.4	10.2	8.44	6.00	3.30	2.04
σ_t	30.9	24.2	18.9	15.2	12.4	10.2	8.44	6.89	4.69	3.66

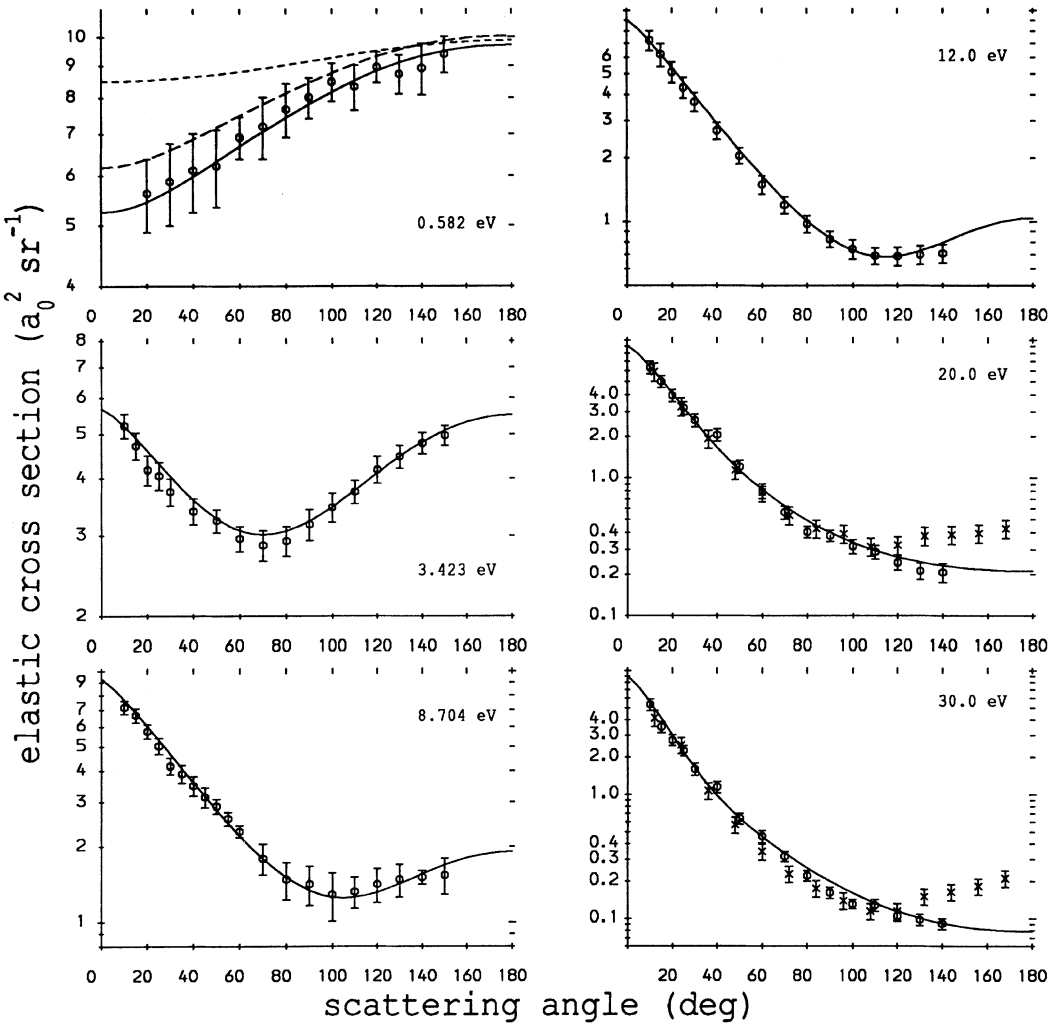

FIG. 2. Elastic differential cross sections. The solid line is the 1CCO calculation. For 0.582 eV the short-dashed line is the static exchange calculation and the long-dashed line is the 1CCO$^-$ calculation, in which Q^+ space is omitted from the polarization potential. The experiments of Williams (Refs. 6 and 7) are denoted by o and those of Shyn and Cho (Ref. 8) by ×.

the 1CCO model with $1s$ in P space and all other states in Q space. The free-particle Green's function was used in Q^+, i.e., f and g in (52) are, respectively, the regular and the irregular Riccati-Bessel functions for Q^+.

The results are in complete agreement with the experiments of Williams.[6,7] We have plotted our results against experiment for some selected energies in Fig. 2. The agreement for other energies is equally good. The experimental results of Shyn and Cho[8] differ from those of Williams at backward angles at 20 and 30 eV. Our theory agrees with that of Williams.

For the smallest calculated energy we also plotted the static exchange (1CC) calculation and the 1CCO$^-$ ($Q = Q^-$) calculation to show the effect of the discrete and continuum parts of the polarization potential separately. The whole polarization potential is necessary to achieve the excellent agreement with experiment even at very low energy.

V. CONCLUSIONS

The CCO theory presented here successfully reproduces the experimentally observed elastic differential cross section and semiempirical estimates of the total cross section for electron-atomic hydrogen scattering at projectile energies of 0.5–30 eV. We have found that it is important to treat both the projectile and the target electron in the polarization potential symmetrically at these energies.

The approximations of the theory are made in the Green's function of the polarization potential, which represents the (essentially unknown) three-body aspects of

Q space. It is hoped that the treatment of P-space channels is sufficiently detailed that agreement with experiment can be achieved with tractable approximations for Q space.

For tractability it is necessary to calculate the Green's function in a local, central potential, thus ignoring coupling of the Q-space channels among themselves. The complete success of the calculation justifies this approximation and shows that the important contributions to the polarization potential come from Q-space channels coupling directly to P-space channels, which is included.

The form used for the local, central potential must represent some kind of kinematic average over the important three-body properties. For Q^- space we use the expectation value of the scattering potential in the relevant discrete state of Q^-. This approximation gives internal consistency[5] in the sense that the results for a particular P space are the same irrespective of whether other discrete states are added to P space or included in Q^- space.

For Q^+ (ionization) space the Coulomb Green's function severely overestimates total reaction cross sections at low energy. The free-particle Green's function gives cross sections within experimental error at the energies considered here and similar results to previous work[1] at higher energies. The expansion of this CCO method to higher atoms in now under investigation.

ACKNOWLEDGMENTS

We would like to acknowledge support from the Australian Research Council. One of us (D. A. K.) acknowledges financial support from The Flinders University of South Australia.

[1] I. Bray, D. H. Madison, and I. E. McCarthy, Phys. Rev. A **41**, 5916 (1990).
[2] B. H. Bransden, T. Scott, R. Shingal, and R. K. Roychoudhury, J. Phys. B **15** 4605 (1982).
[3] M. J. Brunger, I. E. McCarthy, K. Ratnavelu, P. J. O. Teubner, A. M. Weigold, Y. Zhou, and L. J. Allen, J. Phys. B **23**, 1325 (1990).
[4] K. Bartschat, R. P. McEachran, and A. D. Stauffer, J. Phys. B **21**, 2789 (1988).
[5] I. Bray, D. A. Konovalov, and I. E. McCarthy, J. Phys. B (to be published).
[6] J. F. Williams, J. Phys. B **8**, 1683 (1975).
[7] J. F. Williams, J. Phys. B **8**, 2191 (1975).
[8] T. W. Shyn and S. Y. Cho, Phys. Rev. A **40**, 1315 (1989).
[9] M. B. Shah, D. S. Elliot, and H. B. Gilbody, J. Phys. B **20**, 3501 (1987).
[10] F. J. de Heer, M. R. C. McDowell, and R. W. Wagenaar, J. Phys. B **10**, 1945 (1977).
[11] Y. Hahn, T.F. O'Malley, and L. Spruch, Phys. Rev. **128**, 932 (1962).
[12] I. E. McCarthy and A. T. Stelbovics, Phys. Rev. A **28**, 2693 (1983).
[13] I. E. McCarthy and X. Zhang, Aust. J. Phys. **43**, 291 (1990).